

Polymer-free cerivastatin-eluting stent shows superior neointimal inhibition with preserved vasomotor function compared to polymer-based paclitaxel-eluting stent in rabbit iliac arteries

Lakshmana K. Pendyala¹, MD; Xinhua Yin², MD, PhD; Jinsheng Li¹, MD, PhD; Toshiro Shinke¹, MD, PhD, FACC; Yawei Xu¹, MD, FACC; Jack P. Chen¹, MD, FACC; Spencer B. King III¹, MD, MACC; Kenneth Colley³, MD, PhD; Traci Goodchild¹, PhD; Nicolas Chronos¹, MD, FACC; Dongming Hou^{1*}, MD, PhD, FACC

1. Saint Joseph's Translational Research Institute/Saint Joseph's Hospital of Atlanta, GA, USA; 2. The First Affiliated Hospital of Harbin Medical University, Harbin, China; 3. DiaDexus, Inc., South San Francisco, CA, USA

None of the authors have a conflict of interest to declare. This study was supported by a research grant from Medlogics Corporation. The first two authors contributed equally to this work.

KEYWORDS

Cerivastatin, drug-eluting stents, endothelial function

Abstract

Aims: The present study was designed to evaluate vasomotor function and vascular biological responses following a novel non-polymeric cerivastatin-eluting stent (CES) versus polymer-based paclitaxel-eluting stent (PES) in a rabbit iliac artery model. Optimisation of DES components and non-polymeric stents may contribute to vascular healing and beneficial to vasomotor function.

Methods and results: *In vitro* human aortic and coronary smooth muscle cells (hASMC & hCSMC), as well as endothelial cells (hAEC & hCEC) were cultured. IC50 curves were determined for cerivastatin (CER). *In vivo* PES (n=6) and CES (n=12) stents were implanted in nine rabbits. Vasomotor function was investigated at 28 days by acetylcholine (ACh) followed by histopathological and histomorphometric analyses. CER was cytotoxic to hASMC and hCSMC (IC50s of 10⁻⁶ M and 10⁻⁵ M, respectively), although such cytotoxic effects were not observed for hAEC and hCEC at maximal study dose. PES-associated vasodilation response to endothelial-dependent ACh was significantly suppressed at both proximal and distal adjacent arterial segments, as compared to CES. Furthermore, microscopically, neointimal inhibition quantified by the neointimal cross-sectional area (IA) was superior with CES (0.60±0.27 mm²) compared to PES (1.35±0.16 mm²; P <0.05). Medial area was smaller for PES (0.3±0.04 mm²) than CES (0.5±0.03 mm², p <0.001). Additionally, significant inflammation and fibrin deposition was clearly evidenced in PES compared to CES (p <0.05).

Conclusions: CER elicits a differential effect on hSMC compared to hEC *in vitro*. In contrast to PES, a novel bioabsorbable sol-gel coated CES demonstrated effective neointimal inhibition with less vessel wall toxicity accompanied by preservation of vasomotor function in the rabbit iliac model.

* Corresponding author: Saint Joseph's Translational Research Institute/Saint Joseph's Hospital of Atlanta, 5673 Peachtree Dunwoody Rd, Suite 675, Atlanta, Georgia 30342, USA

E-mail: dhou@sjha.org

© Europa Edition 2010. All rights reserved.

Introduction

Paclitaxel, the active component of the paclitaxel-eluting stent (PES), is a potent anti-restenosis compound which acts on cytoskeletal proteins via disruption of the microtubule β -tubulin subunit¹. The first-generation Food and Drug Administration (FDA)-approved PES is coated with the permanent styrene-isobutylene-styrene (SIBS) triblock copolymer. Although the PES polymer is used to achieve optimal drug release kinetics, the compound's non-biodegradable characteristic has raised safety concerns with regards to hypersensitivity, inflammatory reaction, and vasomotor dysfunction²⁻⁴. Recently, human autopsy data further revealed poor re-endothelialisation and delayed arterial healing after PES implantation, potentially resulting in life-threatening late stent thrombosis (LST), a rare but catastrophic event^{5,6}.

Statins used for treatment of hypercholesterolaemia inhibit the enzyme 3-hydroxy-3-methylglutaryl coenzyme A (HMG-CoA) reductase and have many pleiotropic properties, which include the reduction of smooth muscle cell (SMC) proliferation, inhibition of vascular inflammation and platelet activation, and promotion of endothelial cell (EC) growth⁷. To avoid the undesirable and potentially devastating side-effects associated with drug-eluting stents (DES) such as PES, a statin-based stent delivery system has been designed to not only retard restenosis, but more importantly, to promote endothelial regeneration. Silica sol-gel is a bioabsorbable, biocompatible matrix used in medicinal applications for encapsulation of bio-molecules such as enzymes, genes, proteins, and antibodies, and it has been used safely in intraocular lenses⁸. A novel bioabsorbable, polymer-free, thin film sol-gel coating for delivery of cerivastatin (CER) on a thin strut (71 μm) cobalt-chromium (Co-Cr) as stent platform (CES) has recently been developed. Therefore, the present study was designed to evaluate vasomotor function and vascular biological response following CES versus PES in a rabbit iliac artery model.

Methods

In vitro cell culture and cytotoxicity assay

Human aortic and coronary artery SMCs and ECs were purchased commercially (Cell Applications, Inc., San Diego, CA, USA). Cryopreserved vials of cells were thawed, re-suspended in fresh growth medium, and plated in 96-well plates at a density of 5,000 cells/well. Cells were cultured and passaged according to supplier's recommendations. The day prior to experimental treatment, SMCs and ECs were washed with Dulbecco's phosphate buffered saline (dPBS) then cultured in low serum (0.1%) to quiesce the cells for 48 hours.

On the day of experiment, various concentrations of CER (0, 0.39, 0.78, 1.56, 3.13, 6.25, 12.5, 25, 50, 1×10^2 , 2×10^2 , 4×10^2 , 8×10^2 , 16×10^2 , 32×10^2 , 64×10^2 nM) were added to SMCs and ECs with media containing 0.1% serum. After 48 hours of incubation, the cells were rinsed with dPBS and processed for fluorescent evaluation of cytotoxicity. Each concentration of CER was performed in triplicate, and each experiment was done in triplicate plates. Total cytotoxicity was determined using the commercially available MultiTox-Fluor multiplex cytotoxicity assay kit (Promega, Madison,

WI, USA). The MultiTox-Fluor Multiplex Cytotoxicity Assay simultaneously measures the relative number of live and dead cells in cell populations by simultaneously measuring two protease activities of cell viability, and cytotoxicity. The live cell protease activity is restricted to intact viable cells and is measured using a fluorogenic, cell-permeant, peptide substrate (glycyl-phenylalanyl-aminofluorocoumarin; GF-AFC). The substrate enters intact cells where it is cleaved by the live-cell protease activity to generate a fluorescent signal proportional to the number of living cells. This live-cell protease becomes inactive upon loss of cell membrane integrity and leakage into the surrounding culture medium. A second, fluorogenic cell-impermeant peptide substrate (bis-alanylalanyl-phenylalanyl-rhodamine 110; bis-AAF-R110) is used to measure dead cell protease activity, which is released from cells that have lost membrane integrity. Because bis-AAF-R110 is not cell-permeant, essentially no signal from this substrate is generated by intact, viable cells. The live- and dead-cell proteases produce different products, AFC and R110, which have different excitation and emission spectra, allowing them to be detected simultaneously.

Dead-cell fluorescence was determined using excitation at 485 nm and emission at 520 nm (BioTek Synergy 2 plate reader, Gen5 software; BioTek, Winooski, VT, USA). The effect on cell growth was calculated as the difference in relative fluorescence percentage in the presence and absence of cerivastatin and illustrated in a dose-response curve. The concentration at which the growth of cells was inhibited to 50% of the control (IC_{50}) was obtained from this dose-response curve. IC_{50} s were calculated using SigmaPlot software (Systat Software Inc., London, United Kingdom).

Stent characteristics

The sol-gel matrix-coated CES, which has both biocompatible and bioabsorbable properties, were provided by Medlogics Device Corporation (Santa Rosa, CA, USA). The test articles, 2.5 mm in diameter and 12 mm in length, were balloon-expandable stents. The stents were laser-cut from a Co-Cr super-alloy tube, consisting of a series of sinusoidal elements with optimised rounded, sweeping bulb-like crown design to minimise vessel trauma, and were pre-mounted on a custom rapid-exchange balloon. The stent strut thickness was 71 μm with 4 μm thick bio-matrix layer. The CER dose density was 0.22 $\mu\text{g}/\text{mm}^2$, and total dose was 9.94 μg per 12 mm stent. *In vitro* drug release kinetics from the CES was measured in phosphate-buffered saline (PBS) at 37° C at pH 7.4 for 35 days. CER content was measured daily using high-performance liquid chromatography (HPLC) at 238 nm. Elution of CER from CES was a slow-release formulation without an early rapid burst phase. Approximately 70% of total loading dose was released by day three; 90% by day seven; and 96% by day of 21 (Figure 1). Drug amounts released were below the detection limits after day 35. All devices were individually packaged and sterilised by E-beam irradiation before use.

Control group, included FDA-approved PES (TAXUS® Express® stent, 2.5 mm in diameter and 16 mm in length, strut thickness 132 μm and polymer thickness 16 μm , dose density 1 $\mu\text{g}/\text{mm}^2$, with total dose of 108 μg per stent), which was purchased as a commercially available product.

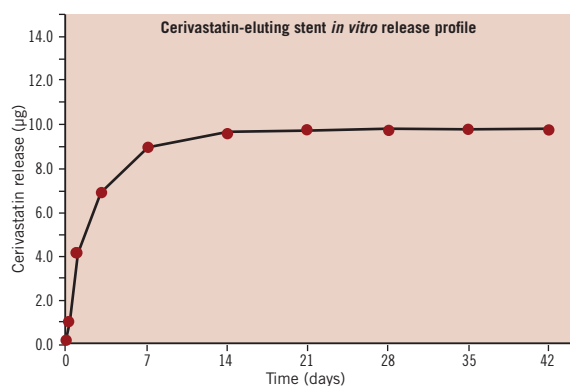


Figure 1. Cerivastatin release kinetics from CES in vitro. CES: cerivastatin-eluting stent.

Animals and experimental protocol

Animal handling and care followed the recommendations of the National Institutes of Health (NIH) guide for the care and use of laboratory animals⁹. All protocols were approved by the Saint Joseph's Translational Research Institute's Animal Care and Use Committee and followed the Association for Assessment and Accreditation of Laboratory Animal Care (AAALAC) guidelines.

A total of 18 stents from two different groups, PES (n=6) and CES (n=12) were implanted in rabbit (3-4 kg) iliac arteries. All animals received 1mg/kg aspirin and 1mg/kg clopidogrel daily for a minimum of three days prior to procedure and daily thereafter until termination. All rabbits were fasted overnight prior to the stent implant procedure. Sedation was accomplished by intramuscular injection of ketamine 35 mg/kg and xylazine 5 mg/kg, followed by maintenance inhalant isoflurane via nose cone delivered at a concentration of 0.5-5% in a mixture of O₂ or N₂O. Electrocardiogram and blood pressure were continuously monitored during stent implantation, angiographic restudy, and vascular function studies.

Catheterisation was performed through carotid cut-down following heparinisation (200 units/kg). After engaging a 5 Fr guide catheter, stents were deployed with two 12 atm for 20 sec inflations bilaterally, which reached about 10-15% S:A ratio. After post-deployment arteriogram confirmed stent apposition and vessel patency, carotid vessel access was closed and animals were allowed to return to cages.

In vivo evaluation of endothelial function

At 28-day follow-up, endothelium-dependent and -independent vasorelaxation of the proximal and distal non-stented reference segments in all stented arteries were assessed after infusion of two incremental doses of acetylcholine (ACh, 10⁻⁶ and 10⁻⁵ mol/L), followed by a single dose of nitroglycerin (NTG, 200 µg) administered via the guide catheter above the iliac bifurcation. ACh was delivered through infusion pump (Harvard Apparatus, Holliston, MA, USA) at 0.8 ml/min for three minutes¹⁰. After a 10-minute interval, intra-arterial NTG was administered as a bolus. Angiography was performed using identical projections before and after drug administration. The percent diameter change from baseline to post-infusion at 5 mm proximal and distal to the stented

segment was considered to reflect vasorelaxation capacity. Animals were terminated after the procedure for complete histopathological and histomorphometric analyses.

Microscopic evaluation

Stented iliac arteries were perfusion-rinsed with 0.9% NaCl solution and perfusion-fixed *in situ* at physiologic pressure with 5% formalin/1.25% glutaraldehyde for 15-20 min, trimmed free from the surrounding tissue, immersed in formalin overnight, and then embedded in methyl methacrylate the following day. Sections from proximal, middle, and distal vessel regions were cut using a heavy-duty microtome equipped with a tungsten-carbide knife, mounted on glass slides, stained with hematoxylin-eosin (H&E) and Verhoeff-Masson (VM) elastic-trichrome stain, and analysed using a computer-assisted image analysis system (Image Pro Plus, Media Cybernetics, Bethesda, MD, USA).

Sections from each of the stent segments were scored for the extent of vessel wall injury, inflammation, intramural fibrin deposition, necrosis of tunica media, and re-endothelialisation. Injury score was evaluated at each stent strut determined by stent strut penetration into the vessel wall where:

- 0 = Internal elastic lamina intact, media compressed but not lacerated;
- 1 = Internal elastic lamina lacerated; media typically compressed but not lacerated,
- 2 = Internal elastic lamina lacerated; media visibly lacerated; external elastic lamina intact, but compressed;
- 3 = External elastic lamina lacerated; typically large lacerations of media extending through the external elastic lamina; stent struts sometimes residing in adventitia.

Inflammation score was assigned according to the following semi-quantitative grading scale:

- 0 = none,
- 1 = mild (scattered inflammatory cells),
- 2 = moderate (inflammatory cells encompassing <50% of a strut in at least 25-50% of arterial circumference),
- 3 = severe (inflammatory cells surrounding a strut in at least 50-75% of arterial circumference).

The same scoring system was used for evaluation of intramural fibrin deposition. Necrosis of the tunica media was scored as:

- 0 = none,
- 1 = mild (focal transmural or non-transmural regions of medial SMC necrosis involving any portion of the artery),
- 2 = moderate (transmural medial SMC necrosis involving >25% of arterial circumference),
- 3 = severe (transmural medial SMC necrosis with involvement of >50% of arterial circumference).

Re-endothelialisation was scored by the circumferential extent of luminal surface coverage in each section with flattened, confluent endothelial or endothelial-like cells as follows:

- 0 = 0-25% coverage of circumference,
- 1 = 25-50% coverage,
- 2 = 50-75% coverage,
- 3 = 75-100% coverage¹¹.

Each vessel section was imaged by a CCD-imaging camera at an appropriate low magnification. Morphometric analysis was performed on the proximal, mid, and distal sections cut from each stented vessel by computerised planimetry using Image Pro Plus software (Media Cybernetics, Bethesda, MD, USA). The lumen, internal elastic lamina (IEL), and external elastic lamina (EEL) were traced; and area measurements obtained. Neointimal and medial areas were obtained by subtraction of the lumen from the IEL and IEL from EEL, respectively. The neointimal thickness at each stent strut site was also measured, and histologic percent area stenosis ($1 - [\text{luminal area}/\text{IEL area}] \times 100$) was calculated.

Statistical analysis

Cell culture data were expressed as mean \pm standard error, and animal experimental data were presented as mean \pm standard deviation. Statistical analysis was performed by SigmaStat version 3.5 (Systat Software, Inc, London, United Kingdom). Changes in iliac diameters in response to drug infusions and histomorphometric data were evaluated by unpaired *t*-test. Histopathologic scoring data were analysed with Mann-Whitney rank sum test. A critical value of $p < 0.05$ was considered significant.

Results

SMC inhibition without influence on EC for both human aortic and coronary cells

CER data from cultured SMC and EC from human aorta and coronary arteries demonstrated dose-dependent growth inhibition

of hSMC cell lines. After a 48 hour incubation period, the IC₅₀ was between 0.8 and 1.6 μM for aortic SMC. In contrast, coronary SMC required higher doses of CER to reach IC₅₀ (3.2 and 6.4 μM) (Figures 2a & b). Importantly, CER, even at the highest concentrations tested, had no effect on hEC from both aorta and coronary arteries (Figures 2c & d).

Comparison of CES- and PES- associated vasomotor function

All animals tolerated the stent implant procedure. There were no stent-related complications or mortalities during the experimental period. Immediate post-procedural and at 28 day follow-up, arteriograms revealed fully patent stent arteries with appropriate sizing and normal brisk forward blood. Both CES and PES stent platforms exhibited similar radio-opacity, which were clearly to visualise under fluoroscopy.

Endothelium-dependent vasomotion was determined by changes in non-stented reference segments iliac diameter from baseline and after ACh infusion. Vasodilatation in response to incremental ACh doses was impaired in PES compared to CES group. The mean iliac diameter change was -14 ± 2 % for PES and 14 ± 4 % for CES at proximal sites ($P < 0.001$); similar patterns were seen at distal sites -17 ± 3 for PES and 10 ± 3 % for CES ($P < 0.001$). In contrast, endothelium-independent relaxation to NTG was comparable between two groups at both proximal (PES 9 ± 2 % vs. CES 14 ± 5 % $P = \text{NS}$) and distal (PES 7 ± 3 versus CES 13 ± 2 % $P = \text{NS}$) sites (Figures 3 & 4a, b).

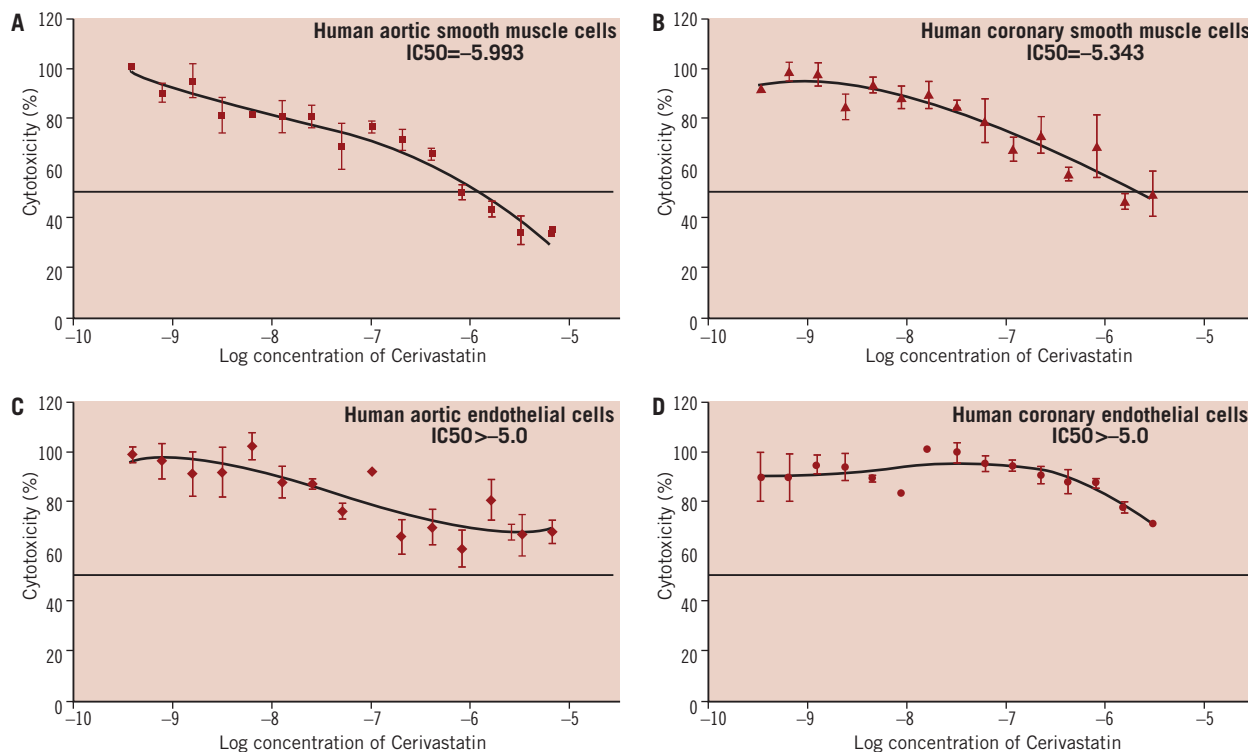


Figure 2. Cytotoxicity concentration curves show that cerivastatin was cytotoxic to varying degrees to all SMC (1a & b) but not to the EC (1c & d). The IC₅₀ was between 0.8 and 1.6 μM for aortic SMC. In contrast, coronary SMC required higher doses of cerivastatin to reach IC₅₀ (3.2 and 6.4 μM). SMC: smooth muscle cells; EC: endothelial cells.

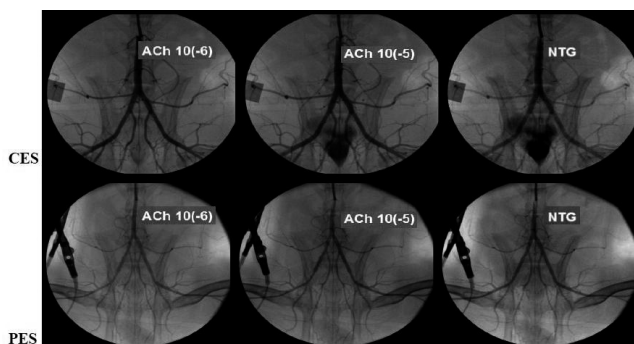


Figure 3. Representative angiographic images in response to endothelial-dependent and -independent relaxation to incremental doses of ACh and nitroglycerin one month after CES and PES implantation. In the PES group, significant diffuse vasoconstriction was induced by ACh in the vessel segments both proximal and distal to the stent. However, the CES group demonstrated no significant vasoconstriction after ACh infusion. Vasodilatory response to nitrates, however, was preserved in both groups. ACh: acetylcholine. NTG: nitroglycerin; PES: paclitaxel-eluting stent.

Microscopic analysis after CES and PES implantation

The stent struts in the both groups were covered by a thin fibrocellular, proteoglycan-rich neointima. Stent apposition was deemed adequate by histology. A complete confluent monolayer of flattened endothelial or endothelial-like cells was seen on the luminal surface for all stents. Scattered inflammatory cells and an occasional foreign body giant cell infiltrate were seen in the peri-strut regions in all stented vessels. Figures 5a & b are illustrative of the microscopic appearance for each stent group.

Moreover, there was no difference in injury score among groups (PES, 1.01±0.13; CES, 0.97±0.21; P=NS). PES exhibited significantly higher histopathologic score for inflammation and peri-strut intramural fibrin deposition compared to CES (P<0.05). Moderate fibrin deposition was found in 23% of PES samples compared to 0% in CES. In contrast, no fibrin deposition was seen in

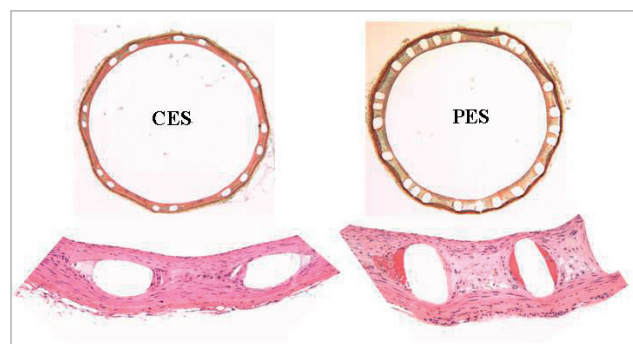


Figure 5. Microscopic images of CES and PES coronary arteries. a, Movat pentachrome staining (20X). b, Hematoxylin & eosin staining (200X). Only in PES, abundant amounts of fibrin deposition was noted. Inflammatory cells in neointima and adventitia were clearly observed too. In contrast, CES exhibited healed fibrocellular neointima with minute deposits of inspissated thrombus and fibrin deposition. Endothelial or endothelial-like cells were completely covered luminal surface in both the stented groups.

35% of CES samples. Similarly moderate inflammation was seen 30% of PES samples compared to 0% in CES samples. Focal medial necrosis subjacent to stent strut profiles was seen in all samples, with PES demonstrating greater focal SMC loss in the tunica media. There were no differences in both medial necrosis and luminal thrombi gradings in any of the stented vessels, and the proximal and distal vessels peri-stent segments were likewise unremarkable. Figure 6 illustrates the histopathologic scoring for each stent group. Histomorphometrically (Table 1), neointimal inhibition was quantified by the neointimal cross-sectional area (IA); the values for CES (0.60±0.27 mm²) were markedly reduced, as compared to PES (1.35±0.16 mm²; P<0.05). Similarly, the percentage of cross-sectional area stenosis (% AS) was also significantly decreased in CES (14.5±6.0%) (16.3±6.5%) compared to PES (25.1±3.0%, P<0.05). There were no significant differences detected in neointimal thickness and luminal area between two groups. Notably, the cross-sectional area of the tunica media (MA) was dramatically decreased

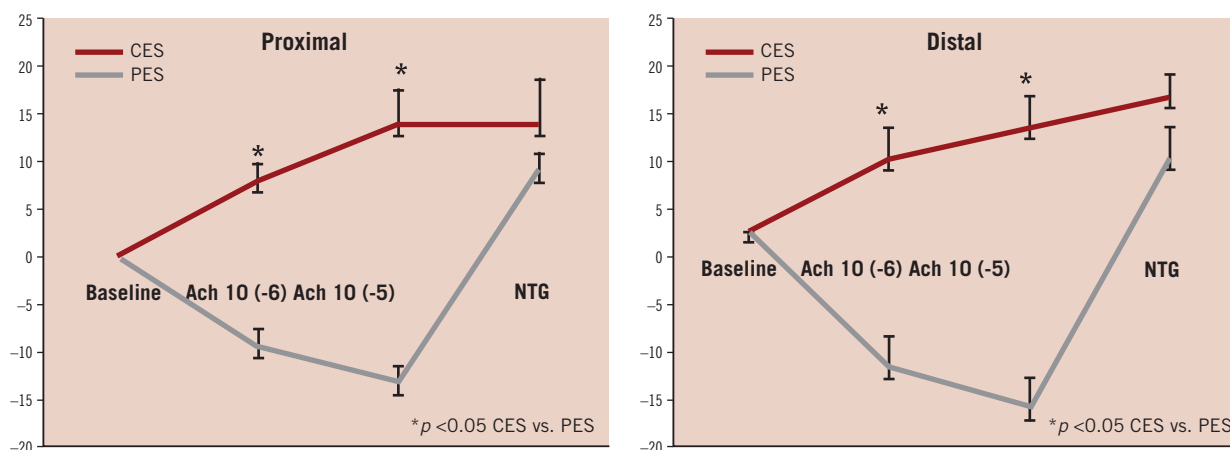


Figure 4. Mean percent diameter change for proximal and distal reference segments in response to ACh and nitroglycerin at one month follow-up. Endothelium-dependent vasodilatory response to ACh was diminished in PES, as compared with CES (P<0.01). However, endothelium-independent response to nitroglycerin was comparable in both the groups (P=NS). NTG: nitroglycerin.

Table 1. Histomorphometric analysis at one month.

	CES	PES	P value
% Lumen stenosis	15±6	25±3*	<0.05
Intimal area (mm ²)	0.60±0.27	1.35±0.16*	<0.05
Lumen area (mm ²)	3.51±0.34	3.96±0.16	NS
Intimal Thickness (mm)	0.06±0.04	0.08±0.01	NS
Elastic lumina area (mm ²)	4.56±0.36	5.61±0.22*	<0.05
Tunica media (mm ²)	0.45±0.03	0.30±0.04*	<0.001

*P <0.05 between PES vs. CES

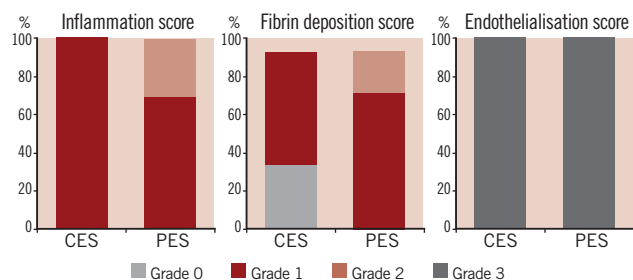


Figure 6. Histomorphopathology showing similar endothelialisation in both the groups; however, inflammation and intramural fibrin score were significantly higher in PES compared to CES ($P < 0.05$ PES vs. CES).

in PES (0.30 ± 0.04 mm²) compared to CES (0.45 ± 0.03 mm²) ($P < 0.001$); the external elastic lamina cross-sectional area (EELA) and the stent area (expressed luminal area plus neointimal area) were significantly greater in PES (5.61 ± 0.22 ; 5.33 ± 0.35 mm²) compared to CES (4.56 ± 0.36 ; 4.12 ± 0.62 mm²) ($P < 0.001$, respectively).

Discussion

We have shown in this study that a novel non-polymeric, silica sol-gel coated CES demonstrated superior neointimal inhibition, reduced vessel wall toxicity as well as preserved vasomotor function in contrast to the FDA-approved first-generation PES at 28 days in rabbit iliac arteries. To the best of our knowledge, this is the first comparison of PES and CES in a pre-clinical rabbit model. Our encouraging findings may have implications for further investigations, with CES and the bioabsorbable silica sol-gel coating, given the growing safety concerns with regards to the first-generation of DES.

CES: benign to EC and preservation of vasomotor function

Consistent with findings of Jaschke et al¹², we demonstrated that *in vitro* CER not only inhibited human aortic, but also coronary SMCs, although the latter required slightly higher dosing. Interestingly, there was no cytotoxic effect observed for both human aortic and coronary ECs, even at the highest doses tested. These findings may suggest beneficial CER cytotoxic specificity for SMCs, mediators of restenosis, while leaving ECs viable and undamaged at the doses tested.

Clinical studies have also shown that oral statins can rapidly improve endothelial function and increase the availability of nitric oxide only days after therapy initiation. Data also suggests that these statin-associated benefits are mediated by reduction of oxidative

stress in the vasculature¹³. In preclinical and clinical settings, statins have also exhibited many other pleiotropic functions such as inflammation reduction, inhibition of platelet activation, and atherosclerotic plaque stabilisation, in addition to lipid lowering¹⁴⁻¹⁶. CER has been shown to be the most potent and efficacious statin for direct inhibition of vascular SMC proliferation¹⁷. While there is evidence that these pleiotropic effects are common to the entire class of statin drugs, cerivastatin achieves these effects at doses 10-100 times lower than other statins.

Therefore, based on its well-documented pro-healing properties, as well as its exceptional pharmacological potency, we considered CER the optimal candidate drug for the next generation of DES. CES demonstrates favourable vascular healing including less vessel wall toxicity and preservation of vasomotor function. Indeed, such effects were clearly evidenced in the present study. Our findings further confirmed those of two other recent pre-clinical studies using rat and swine models^{12,18}. Both studies suggest that CES results in significantly reduced neointimal area with equivalent endothelial coverage at one month, when compared with its bare metal counterpart. Of note, even when using the currently marketed clinical PES as a comparator, we found the neointima area in CES implanted arteries was decreased by 42% compared to commercially available PES.

PES and vasomotor dysfunction

It has been shown that high-dose paclitaxel inhibits both SMC and EC proliferation and migration in cell culture¹. Shin and colleagues¹⁹ studied endothelial function in patients without angiographic evidence of restenosis 6-months following either PES or BMS implantation. Consistent with our findings, the authors reported similar abnormal endothelium-dependent ACh-induced coronary vasoconstriction in the long distal portion (distal and far distal segments) of the treated vessel, with preservation of endothelium-independent vasodilatation.

The mechanisms of endothelial functional impairment following PES implantation remain unanswered. Multiple factors may be involved including, direct toxic effects from the entrapped drug and/or an acute or delayed hypersensitivity reaction from the polymer and/or drug. As recently shown, the *vasa vasorum interna* in coronary arteries, originating directly from the arterial lumen, can extend over several centimetres along the coronary artery wall²⁰. Therefore, the anti-proliferative drugs and vasoactive chemicals may locally diffuse through these micro-channels to the non-stented reference segments. We further demonstrated that localised surface inflammation response at the overlapping PES stent site, as well as increased O₂ production, may be key factors associated with vasomotor dysfunction following overlapping PES implantation in a swine coronary model²¹. Normal vasomotor functioning of the artery is dependent upon normal vasodilatory function via eNOS and nitric oxide pathways, which can be significantly impaired by reactive oxygen species.

Therefore, delayed arterial healing, poor-endothelialisation, and endothelial functional impairment following DES have all been postulated as contributory to the pathogenesis of stent thrombosis²². When compared to CES stents in the present study,

vessel wall toxicity and vasomotor dysfunction with PES were clearly apparent. First, presence of significantly higher inflammatory response and peri-strut fibrin deposition (amorphous material and red blood cell debris) was in PES compared to CES. Secondly, the intramural peri-strut fibrin was also a direct and compelling evidence for delayed vessel wall healing. Furthermore, the medial area was significantly decreased, while the cross-sectional area of elastic lamina tunica was significantly increased. Therefore, the vessel wall toxicity of PES could be expressed as loss of SMC mass due to radial strain in the tunica media, which may further induce the enlargement of EELA. Indeed, diminishing medial area could translate into positive vascular remodelling following PES implantation; this phenomenon may be a sign of drug and/or polymer toxicity response. Loss of the medial layer and late acquired positive remodelling have been reported to result in late stent malapposition clinically, a frequent finding in patients with late/very late DES thrombosis.

Our results further echo those of Pires and associates²³, who demonstrated that high doses of paclitaxel significantly increased apoptosis and internal elastic lamina disruption, while decreasing medial and intimal SMC and collagen content. Moreover, transcriptional analysis by real-time RT-PCR showed an increased level of pro-apoptotic mRNA transcripts (FAS, BAX, caspase 3) in paclitaxel-treated arteries. Finally the luminal diameters at both proximal and distal sites of PES were diminished in response to ACh. Paradoxical pathophysiological vasoreactivity may increase the vulnerability of DES-stented arteries to late/very late stent thrombosis via exacerbation of flow stasis through reduction of laminar flow and flow velocity. Such conditions also would be expected to promote a prothrombotic milieu²².

Study limitations

The first, the length of stent between the groups is different though such a minimal difference in stent length is unlikely to affect the reported study outcomes. The second, utilisation of thin Co-Cr struts as the stent platform for CES; since the extent of vessel wall injury and subsequent SMC proliferation may be proportional to the stent strut thickness²⁴. Thirdly, due to budget limitation, no related bare metal stent or polymer coating stent was used in this pilot study. Therefore, further study is needed to validate our current results. Fourthly, the serum lipid levels were not measured to observe the systemic effects of the statins. We also did not perform *in vivo* pharmacokinetics, which may have provided correlative information to our histologic observations and *in vitro* drug release measurements. Lastly, as our comparator was a first-generation PES, the relative benefits of CES versus other first, as well as second generation, DES remains unknown.

Conclusions

Our findings demonstrate that a novel non-polymeric CES, when compared to the first-generation FDA approved PES, has shown effective neointimal inhibition and significantly less vessel toxicity along with preservation of vasomotor function in the rabbit iliac model. Further work is required to support long-term safety and efficacy of this technology, as well as its clinical applicability.

Acknowledgements

The authors express gratitude to Sara Geva, Cynthia Baranowski and Lian Dorsey for their excellent technical assistance in preparation and reading of the histologic sections, as well as to Lisa Godwin for her technical assistance in the smooth muscle and endothelial cell cultures. We also acknowledge the dedicated assistance of Irena Brants, DVM in managing the study execution.

References

1. Axel DI, Kunert W, Göggelmann C. Paclitaxel inhibits arterial smooth muscle cell proliferation and migration *in vitro* and *in vivo* using local drug delivery. *Circulation* 1997;96:636–645.
2. Chen JP, Hou D, Pendyala L, Goudevenos J A, Kounis NG. Drug-eluting stent thrombosis: the Kounis syndrome revisited. *J Am Coll Cardiol Intv* 2009;2:583–593.
3. Nebeker JR, Virmani R, Bennett CL. Hypersensitivity cases associated with drug-eluting coronary stents: a review of available cases from the Research on Adverse Drug Events and Reports (RADAR) project. *J Am Coll Cardiol* 2006;47:175–181.
4. Kounis NG, Kounis GN, Kouni SN, Soufras GD, Niarchos C, Mazarakis A. Allergic reactions following implantation of drug-eluting stents: A manifestation of Kounis syndrome? *J Am Coll Cardiol* 2006;48: 592–593.
5. Joner M, Finn AV, Farb A, Mont EK. Pathology of drug-eluting stents in humans: delayed healing and late thrombotic risk. *J Am Coll Cardiol* 2006;48:193–202.
6. Finn AV, Nakazawa G, Joner M, Kolodgie FD, Mont EK, Gold HK, Virmani R. Vascular responses to drug eluting stents: importance of delayed healing. *Arterioscler Thromb Vasc Biol* 2007;27:1500–1510.
7. Fukumoto Y, Libby P, Rabkin E. Statins alter smooth muscle cell accumulation and collagen content in established atheroma of Watanabe heritable hyperlipidemic rabbits. *Circulation* 2001;103:993–999.
8. Coradin T, Boissiere M, Livage J. Sol-gel chemistry in medicinal science. *Curr Med Chem* 2006;13:99–108.
9. Schwartz RS, Edelman ER, Carter A. Drug-eluting stents in preclinical studies: recommended evaluation from a consensus group. *Circulation* 2002;106:1867–1873.
10. Schwarzacher SP, Lim TT, Wang B, Kernoff RS, Niebauer J, Cooke JP, Yeung AC. Local intramural delivery of L-arginine enhances nitric oxide generation and inhibits lesion formation after balloon angioplasty. *Circulation* 1997;95:1863–1869.
11. Shinke T, Geva S, Pendyala L. Low-Dose Paclitaxel Elution by Novel Bioerodible Sol-gel Coating on Stents Inhibits Neointima with Low Toxicity in Porcine Coronary Arteries. *Int J Cardiol* 2009;135:93–101.
12. Jaschke B, Michaelis C, Milz S. Local statin therapy differentially interferes with smooth muscle and endothelial cell proliferation and reduces neointima on a drug-eluting stent platform. *Cardiovasc Res* 2005;68:483–489.
13. John S, Schneider MP, Delles C, Jacobi J, Schmieder RE. Lipid-independent effects of statins on endothelial function and bioavailability of nitric oxide in hypercholesterolemic patients. *Am Heart J* 2005;149:473–481.
14. Sakai M, Kobori S, Matsumura T. HMG-CoA reductase inhibitors suppress macrophage growth induced by oxidized low density lipoprotein. *Atherosclerosis* 1997;133:51–59.
15. Scalia R, Gooszen ME, Jones SP. Simvastatin exerts both anti-inflammatory and cardioprotective effects in apolipoprotein E-deficient mice. *Circulation* 2001;103:598–603.

16. Huhle G, Abletshauser C, Mayer N, Weidinger G, Harenberg J, Heene DL. Reduction of platelet activity markers in type II hypercholesterolemic patients by a HMG-CoA-reductase inhibitor. *Thromb Res* 1999;95:229–234.
17. Bellosta S, Bernini F, Ferri N, Quarato P, Canavesi M, Arnaboldi L, Fumagalli R, Paoletti R, Corsini A. Direct vascular effects of HMG-CoA reductase inhibitors. *Atherosclerosis* 1998;137:S101-109.
18. Miyauchi K, Kasai T, Yokayama T. Effectiveness of statin-eluting stent on early inflammatory response and neointimal thickness in a porcine coronary model. *Circ J* 72:832-8, 2008.
19. Shin DI, Kim PJ, Seung KB. Drug-eluting stent implantation could be associated with long-term coronary endothelial dysfunction. *Int Heart J* 2007;48:553-67.
20. Gössl M, Rosol M, Malyar NM. Functional anatomy and hemodynamic characteristics of vasa vasorum in the walls of porcine coronary arteries. *Anat Rec A Discov Mol Cell Evol Biol* 2003;272:526–37.
21. Pendyala LK, Li J, Shinke T. Endothelium-dependent vasomotor dysfunction in pig coronary arteries with Paclitaxel-eluting stents is associated with inflammation and oxidative stress. *J Am Coll Cardiol Intv* 2009;2:253-62.
22. Pendyala LK, Yin X, Li J, Geva S, et al. The First-generation Drug-eluting Stents and Coronary Endothelial Dysfunction. *J Am Coll Cardiol Intv* 2009;2:1169-1177.
23. Pires NM, Eefting D, de Vries MR, Quax PH, Jukema JW. Sirolimus and paclitaxel provoke different vascular pathological responses after local delivery in a murine model for restenosis on underlying atherosclerotic arteries. *Heart* 2007;93:922-7.
24. Pache J, Kastrati A, Mehilli J, et al. Intracoronary stenting and angiographic results: strut thickness effect on restenosis outcome (ISAR-STERO-2) trial. *J Am Coll Cardiol* 41:1283-88, 2003.